Acta Neurologica Belgica (2022) 122:597–613
https://doi.org/10.1007/s13760-022-01943-y

REVIEW ARTICLE

Brainstem lesions: MRI review of standard morphological sequences

Dimitri Renard[1] · Jean-Sebastien Guillamo[1] · Ioana Ion[1] · Eric Thouvenot[1,2]

Received: 29 July 2021 / Accepted: 23 March 2022 / Published online: 15 April 2022
© The Author(s) under exclusive licence to Belgian Neurological Society 2022

Abstract
MRI signal changes in the brainstem are observed in a multitude of disorders including vascular diseases, neoplastic lesions, degenerative diseases, inflammatory disorders, metabolic diseases, infections, and trauma. In some diseases, brainstem involvement is typical and sometimes isolated, while in other diseases, brainstem lesions are only observed occasionally in the presence of other typical extra-brainstem abnormalities. In this review, we will discuss the MRI characteristics of brainstem lesions observed in different disorders associated with frequent and less frequent brainstem involvement. Identification of the origin of the brainstem lesion depends on the exact localisation of the lesion(s) inside the brainstem, the presence and the characteristics of associated lesions seen outside the brainstem, the signal changes on different MRI sequences, the evolution over time of the radiological abnormalities, the history and clinical state of the patient, and other radiological and non-radiological examinations.

Keywords Brainstem · MRI

Introduction

The brainstem as the most caudal part of the brain, connects the cerebrum of the brain to the spinal cord and cerebellum, and is composed of the midbrain, pons, and medulla oblongata. The brainstem is composed of densely packed white (including axons of nerves traversing their ascending or descending course to different structures) and grey matter (including nerve cell bodies for ten of the twelve cranial nerves, pontine nuclei, and reticular formation), playing an important role of regulating cardiac and respiratory function, consciousness, and sleep.

Due to the critical localisation of the brainstem containing various brain substructures, brainstem lesions are often associated with multiple, often severe, neurological symptoms (including long tract signs, cranial nerve deficit, and cerebellar signs). MRI is a powerful tool to analyse brainstem lesions. T1- and T2-weighted imaging, FLAIR, T2*-weighted imaging, diffusion-weighted imaging, and gadolinium-enhanced T1-weighted images are essential to analyse brainstem lesions in detail. Additional advanced MRI sequences (e.g. perfusion-weighted imaging [PWI], MR spectroscopy [MRS], and diffusion tensor imaging [DTI]) may be useful in some of these disorders. Axial, sagittal, and coronal images give information on the precise localisation of the brainstem lesion. In this review, we will focus on the MRI characteristics of brainstem lesions encountered frequently or less frequently in the different disorders on standard morphological MRI sequences. We present a table showing an overview of the MRI characteristics of the brainstem lesions frequently encountered in the different disorders (Table 1).

Vascular lesions

Infarction

Main arterial trunks supplying the brainstem include the vertebral, anterior spinal, posterior inferior cerebellar, basilar, anterior inferior cerebellar, superior cerebellar, posterior cerebral, posterior communicating, and anterior choroidal arteries. The collaterals of these arteries are divided into four

✉ Dimitri Renard
dimitrirenard@hotmail.com

[1] Department of Neurology, CHU Nîmes, Hôpital Carémeau, University of Montpellier, 4 Rue du Professeur Debré, 30029 Nîmes Cedex 9, France

[2] Institut de Génomique Fonctionnelle, CNRS UMR5203, INSERM 1191, University of Montpellier, Montpellier, France

Table 1 MRI characteristics of brainstem lesions in different disorders

	T1-weighted imaging	T2-weighted imaging	FLAIR	DWI	ADC	T2*-weighted imaging	Gadolinium injected T1 imaging
Acute infarction	↓ (→ in hyperacute phase)	↑ (→ in hyperacute phase)	↑ (→ in hyperacute phase)	↑	↓		−
Chronic infarction	↓	↑	↑	↑ (T2 effect) or ↓ (lacuna)	↑		−
CHSVD	→↓	↑	↑	↑ (T2 effect) or ↓ (lacuna)	↑	↓ (blood products)	−
Acute ICH	↑ (→ in hyperacute phase)	↑↓ (depending on stage)	↑↓ (depending on stage)	↑↓ (mixed)	↑↓ (mixed)	↓	(+)
CM	↑↓ mixed	↑↓ mixed	↑↓ mixed	↑↓ (mixed in acute bleeding)	↑↓ (mixed in acute bleeding)	↓	(+)
DAF-related oedema	→↓	↑	↑	↑↓	↑↓		(+)
DVA	↓ (flow void)	↓ (flow void)	↓ (flow void)	→	→	↓	+(vessels)
DPVS	↓	↑	↓	→	→	↓	(+) (penetrating arteries)
Glioma	↓	↑	↑	(↑)	(↓)	(↓) (neovascularisation or blood products)	(+)
CNS lymphoma	→↓	↓→	↓→	(↑)	(↓)	(↓) (blood products)	+(intense, diffuse)
Hemangioblastoma	↓	↑	↑	(↓) (cystic portion)	↑ (cystic portion)	(↓) (blood products)	+(nodule)
Ependymoma	→↓	↑→	↑→	→	→	(↓) (calcifications, blood products)	+(mild/moderate, heterogeneous)
Metastasis	→↓	↑→	↑→	→	→	(↓) (blood products, melanoma)	+(nodular, ring-like)
MSA	→	↑	↑	→	→	↑	−
DRPLA	→↓	↑	↑	→	→		−
MS	→↓	↑	↑	(↑) (acute lesion)	(↓) (acute lesion)	(↓) (central vein)	(+) (acute lesion)
SS	→↓	↑	↑	→	→		−
NMOSD	→↓	↑	↑	(↑)	(↓)		(+)
ADEM	→↓	↑	↑	(↑)	(↑)		+(all or nearly all lesions)
NBD	→↓	↑	↑	(↑)	(↓)		(+)
CLIPPERS	→↓	↑	↑	→	→		+
ODS	→↓	↑	↑	(↑)	(↑↓)		−
WE	→↓	↑	↑	(↑)	(↓)	(↓) (rare, blood products)	(+)
PRES	→↓	↑	↑	(↑)	(↑)	(↓) (rare, blood products)	(+)
LS	↓	↑	↑	(↑)	(↓)		−
WD	↓(↑)	↑(↓)	↑	(↑) (in acute phase)	(↓) (in acute phase)		−

Table 1 (continued)

	T1-weighted imaging	T2-weighted imaging	FLAIR	DWI	ADC	T2*-weighted imaging	Gadolinium injected T1 imaging
Leukodystrophy	→↓	↑	↑	→	→		−
Wallerian degeneration	→↑↓	→↓↑	→↓↑	(↑) (in early phase)	(↓) (in early phase)		−
HOD	→↓	↑	↑	→	→		−
ALS	→	↑	↑	(↑)	→		−
IRE	→↑↓(depending on agent and stage)	→↑↓ (depending on agent and stage)	→↑↓ (depending on agent and stage)	→↑	→↓↑		+
PML	↓	↑	↑	(↑)	→		−
DAI	→	↑	↑	↑	→↓↑	↓ (blood products)	−

	Other useful MRI sequences/techniques	Brainstem localisation	Lesion aspect	Other useful radiological CNS abnormalities outside the brainstem
Acute infarction	PWI		Vascular territory, diffuse, uni- or multifocal	Arterial occlusion on MRA/CTA
Chronic infarction			Vascular territory, diffuse, uni- or multifocal	Possible secondary WD
CHSVD		Pons	Wmh in lemniscus medialis	BG WMH/DPVS/CMB; dolichoectasia
Acute ICH		Midbrain/pons		intraventricular haemorrhage; chronic AHT signs (if AHT -related); CM (if CM-related)
CM	SWI	Pons		DVA; calcification on CT
DAF-related edema	Time-resolved imaging of contrast kinetics for DAF imaging			Vascular flow voids
DVA			Medusa head vessels	Signal changes related to infarction or hemorrhage; CM
DPVS	Hydrographic 3D high-resolution turbo spin-echo with variable flip angle		Oval, round, or tubular	
Glioma	PWI	Pons > midbrain	Diffuse, sometimes cystic	Calcifications (midbrain tectal glioma), mass effect, hydrocephalus
CNS lymphoma	PWI			
Hemangioblastoma			Cyst with mural nodule > solid hypervascular lesion	Vascular flow voids
Ependymoma			Surrounding the fourth ventricle, irregular	Calcifications, cysts, haemorrhage
Metastasis	PWI		Unique or multiple	
MSA		Pons	Hot cross-bun sign	Other MSA-related brain abnormalities
DRPLA		Midbrain/pons		other DRPLA-related brain abnormalities
MS	SWI (to detect central vein)	Pons > midbrain > medulla	Round or ovoid, sometimes linear (e.g. Trigeminal)	other MS-related brain and spinal cord lesions
SS		Medulla > pons	Round or ovoid, solitary	
NMOSD		Midbrain/pons	Peri-ependymal areas, corticospinal tracts	Other NMOSD-related brain and extensive spinal cord lesions

Table 1 (continued)

	Other useful MRI sequences/techniques	Brainstem localisation	Lesion aspect	Other useful radiological CNS abnormalities outside the brainstem
ADEM				other ADEM-related lesions
NBD		Midbrain/pons		Brainstem lesion often extending upwards to the diencephalon and basal ganglia
CLIPPERS		Pons > midbrain/medulla	Multiple, small, punctuate or curvilinear	
ODS		Pons > midbrain/medulla	Bilateral, symmetrical; trident-, wing- or eagle-like	Extrapontine ODS lesions
WE		Midbrain/medulla	Bilateral; periaqueductal, medial vestibular nuclei	Involvement of mammillary bodies, medial thalamus, perirolandic regions
PRES		Pons > midbrain/medulla	Diffuse, with swelling	Signal changes related infarction or haemorrhage, WMH in posterior brain regions
LS	MRS	Midbrain/medulla > pons	Bilateral symmetrical	
WD		Pons > midbrain/medulla	Bilateral symmetrical	Other (especially BG) WD lesions
Leukodystrophy			Depending on type of leukodystrophy	Diffuse supratentorial WMH
Wallerian degeneration				Initial brain injury causing Wallerian degeneration
HOD		Medulla	Uni- or bilateral	Initial brain injury causing HOD
ALS	DTI		Bilateral symmetrical	Precentral cortical hypointensities on T2*/SWI
IRE				Leptomeningeal involvement (FLAIR ↑ and gadolinium enhancement)
PML		Pons > midbrain/medulla	Unique or multiple	Extra-brainstem PML lesions
DAI	SWI	Midbrain/pons > medulla	Multifocal	Other radiological manifestations of head trauma

CHSVD, chronic hypertensive small vessel disease; ICH, intracerebral haemorrhage; CM, cavernomatous malformation; DAF, dural arteriovenous fistula; DVA, developmental venous anomaly: DPVS, dilated perivascular spaces; CNS, central nervous system; MSA, multiple system atrophy; DRPLA, dentatorubral-pallidoluysian atrophy; MS, multiple sclerosis; SS, solitary sclerosis; NMOSD, neuromyelitis optica spectrum disorder; ADEM, acute disseminated encephalomyelitis; NBD, neuro-Behçet's disease; CLIPPERS, chronic lymphocytic inflammation with pontine perivascular enhancement responsive to steroids; ODS, osmotic demyelination syndrome; WE, Wernicke encephalopathy; PRES, posterior reversible encephalopathy syndrome; LS, Leigh syndrome; WD, Wilson disease; HOD, hypertrophic olivary degeneration; ALS, amyotrophic lateral sclerosis; IRE, infectious rhombencephalitis; PML, progressive multifocal leukoencephalopathy; DAI, diffuse axonal injury; FLAIR, fluid-attenuated inversion recovery; DWI, diffusion-weighted imaging; ADC, attenuated diffusion coefficient; PWI, perfusion-weighted imaging; SWI, susceptibility-weighted imaging; MRS, magnetic resonance spectroscopy; DTI, diffusion tensor imaging; WMH, white matter hyperintensities; MRA, magnetic resonance angiography; CTA, computed tomography angiography, BG, basal ganglia; CMB, cerebral microbleeds; AHT, arterial hypertension

(i.e. anteromedial, anterolateral, lateral, and posterior) arterial groups. The origin of arterial supply varies at each brainstem level [1]. The location of the brain infarction essentially depends on the artery involved. Occlusion of the proximal and middle portion of the basilar artery is most often caused by an occlusive thrombus related to large artery atherosclerosis, whereas distal basilar artery occlusion is most often associated with cardiac or artery-to-artery embolism.

In acute brainstem infarction, unenhanced CT is not sensitive and most often normal except for the presence of a hyper-dense artery sign in case of vertebrobasilar artery occlusion, whereas CT angiography will show the steno-occlusive vertebral and/or basilar artery lesion [2, 3]. Acute brainstem infarction is best visualised on diffusion-weighted imaging showing restricted diffusion (i.e. increased signal on DWI and decreased signal on ADC map) while T2-weighted and FLAIR imaging showing increased signal only in the late acute phase (Fig. 1 and Supplementary Fig. 1). In a minority of cases, diffusion-weighted imaging is normal in the acute phase and has to be repeated to confirm brainstem infarction [4]. When certain branches (typically unilateral) of the vertebral or basilar artery are involved, specific brainstem involvement (and associated neurological syndrome) can be observed (e.g. infarction of the lateral medulla oblongata, para-median or lateral pontine structures, or the midbrain) (Supplementary Fig. 1). Basilar artery occlusion typically causes large (often asymmetric or multifocal) brainstem infarctions (Fig. 1), whereas lacunar infarctions are typically small and unique. In case of basilar artery occlusion, associated lesions involving the thalamus, occipital lobe, mesial temporal lobe, or splenium (all depending of the posterior cerebral artery) are often observed (Fig. 1). Perfusion-weighted imaging (PWI) is considered unreliable for brainstem stroke, although associated large cerebellar hemispheric hypo-perfusion can be observed in case of involvement of one of the cerebellar arteries. MRA can be used to show steno-occlusive lesions of the vertebral and basilar arteries and their main trunks while smaller penetrating arteries cannot be visualised on these images. Chronic infarction is typically seen as a hyper-intensity on T2-weighted and FLAIR imaging, sometimes associated with a cerebrospinal fluid-filled cavity (hyper-intense on T2 and hypointense on FLAIR imaging) within the hyperintensity (lacuna).

After infarction, a process of Wallerian degeneration (cfr infra) can be sometimes observed as a T2/FLAIR hyperintensity involving the corticospinal, pontocerebellar, and the dentate-rubro-olivary pathways in the brainstem.

Chronic hypertensive small vessel disease

Chronic hypertensive small vessel disease (CHSVD) is characterised by lacunar infarcts (defined as 3–15 mm cerebrospinal fluid-filled cavities), white matter hyper-intensities, enlarged perivascular spaces, cerebral micro-bleeds and intracerebral haemorrhage (ICH) [5]. CHSVD is often associated with the presence of vertebrobasilar dolichoectastia. Lacunar infarcts and white matter hyper-intensities typically involve the deep grey matter, internal and external capsules, and the brainstem. In the brainstem, CHSVD-related white matter T2/FLAIR hyper-intensities are often bilateral, can be symmetric or asymmetric, confluent or multifocal, and typically involve the pons and particularly the medial lemniscus (Supplementary Fig. 2) [6, 6]. In CHSVD, dilated perivascular spaces are typically seen in the deep brain structures, and cerebral micro-bleeds and ICH in the basal ganglia (or show mixed cortical and deep location), the brainstem or the deep cerebellum (nucleus dentatus).

Intracerebral haemorrhage

Brainstem localisation can be observed in 5–10% of patients with ICH. Brainstem ICH, typically associated with hypertension, most frequently involves the pons or the midbrain. [8, 9]. Because of the proximity of the fourth ventricle, brainstem ICH is often associated with intraventricular haemorrhage.

On CT, acute ICH is typically seen as a round or elliptical parenchymal well-delineated hyperdensity. In the subacute phase, borders become less delineated, ICH density

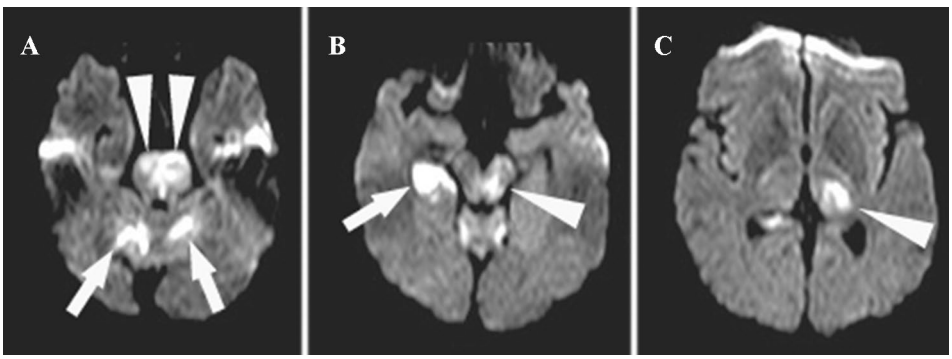

Fig. 1 In a patient with proximal basilar artery occlusion, DWI-weighted imaging shows bilateral pontine (**A**, arrowhead) and cerebellar (**A**, arrows), right-sided mesial temporal (**B**, arrow) and left-sided mesencephalic (**B**, arrowhead), and left thalamic (**C**, arrowhead) infarction

decreases, and surrounding low density oedema often occurs. On MRI, diffusion-weighted imaging typically show mixed hyper/hypointense signal, whereas signals on T1, T2, and FLAIR imaging depend on the timing of imaging. In case of acute and active haemorrhage, a so-called "spot sign" (considered as radiological biomarker for rapid ICH growth) can be seen when contrast enhancement inside the ICH is present on gadolinium-enhanced T1-weighted imaging. In both the acute and chronic bleeding phase, prominent susceptibility effect, seen as hypointense "blooming" on T2*- and susceptibility-weighted imaging (SWI) is typically seen.

Cavernomatous malformation

Overall, brainstem localisation is observed in 14% of patients with cavernous malformations (CM), in 8% in case of incidental presentation, in 32% of CM presenting with ICH or focal neurological deficit, and absent in case of presentation with seizures. The pons is the most frequent localisation in case of brainstem CM. CMs typically do not enhance on contrast-enhanced CT or T1-weighted MR imaging, although slight enhancement may sometimes be observed. Associated developmental venous anomaly (DVA) can be observed in 14–34% of CM, generally well visualised on contrast-enhanced CT or MRI. On CT, CM with recent bleeding is visualised as hyper-density in the acute and subacute phases. Since CM often shows calcification (associated with very high densities on CT), the presence of calcification may help to identify CM as cause of the recent bleeding. On MRI, T1/T2/FLAIR imaging typically shows mixed intensities due to the presence of mixed recent and chronic haemorrhage and frequently associated calcification, with often a so-called "popcorn" aspect (Supplementary Fig. 3). CMs are best detected on T2* and SWI imaging, seen as hypointensities (Supplementary Fig. 3). SWI is more sensitive than T2*-weighted imaging in detecting CM, especially in familial CM often associated with multiple CM (Supplementary Fig. 3). Infra-tentorial CM location, the presence of DVA, and large CM (> 1 cm^3) are associated with high bleeding risk [10–12].

Dural arteriovenous fistula

In decreasing order of frequency, the most common localisations of dural arteriovenous fistula (DAF) are the craniocervical junction, cavernous sinus, superior petrosal sinus, transverse or sigmoid sinus, tentorium, and other sites. DAF sometimes leads to signal changes in the brainstem related to congestive venous oedema secondary to arterial pressure via the fistula [13]. Brainstem signal is increased on T2-weighted imaging and FLAIR sequences, hypo- or isointense on T1-weighted imaging, and variable on DWI. Contrast enhancement on gadolinium-injected T1-weighted imaging is observed in the majority of patients. Mass effect due to congestive oedema and the presence of gadolinium enhancement may mimic brainstem tumour. Vascular flow void can be seen in most patients. In uncomplicated DAF, susceptibility effect is often absent on T2*-weighted imaging and SWI. In patients with brainstem engorgement, angiography shows stenosis or occlusion of the draining system distal to the fistula points. Treatment by occlusion of DAF typically leads to resolution of brainstem oedema.

Developmental venous anomaly

Developmental venous anomaly (DVA) represents a congenital variant of the normal drainage, composed of dilated veins giving the so-called aspect of "medusa head" (stellate tubular vessels converging on collector vein), with the collector vein (the central pontine vein or the vein of the lateral recess of the fourth ventricle vein in case of posterior fossa DVA) draining into petrosal sinuses. Flow voids can be seen on different MRI sequences. T2*-weighted imaging and SWI are especially interesting in case of associated CM giving a susceptibility (so-called "blooming") effect. Most DVAs are asymptomatic and incidentally found on neuroimaging studies. Neurological manifestations sometimes observed are associated with thrombus formation and oedema resulting from DVA thrombosis, or in case of compression caused by the main collector vein (e.g. compression of the root entry zone of the facial nerve causing hemi-facial spasm) [14].

Dilated perivascular spaces

Perivascular (also known as Virchow–Robin) spaces (PVS) are pial-lined, fluid-filled structures surrounding the walls of arteries, arterioles, veins, and venules as they course from the subarachnoid space to the brain parenchyma, as a part of the glymphatic system. They are best visualised on MRI, especially when dilated, and are typically seen as well-defined oval, rounded, or tubular structures with smooth margins, often observed in clusters, and with a range of different sizes [15, 16]. Since PVS are filled with interstitial fluid, signal intensities are identical to CSF on all sequences. Most PVS observed on MRI are incidental findings. Brainstem PVS are categorised as type III PVS, appearing in the midbrain at the pontomesencephalic junction surrounding penetrating branches of the collicular and accessory collicular arteries (Supplementary Fig. 4). Dilated PVS are associated with several small vessel disease-related factors and imaging biomarkers [17]. Sometimes, PVS can become markedly dilated (with or without mass effect), mimicking the appearance of cystic neoplasm. Giant midbrain PVS may compress the aqueduct causing hydrocephalus.

Neoplastic lesions

Glioma

Brainstem glioma accounts for about 20% of paediatric and less than 2% of adult primary brain neoplasms. Since biopsy or surgery is rarely performed because of intervention-related risks, brainstem gliomas are classified radiologically in children into diffuse intrinsic pontine glioma and focal glioma, and in adults into diffuse intrinsic low-grade glioma, enhancing malignant glioma, and midbrain tectal glioma [18]. Contrast enhancement is often absent in paediatric patients, whereas a variable degree of enhancement is observed in adult brainstem glioma patients. Overall, the most frequent brainstem location is the pons. Midbrain tectal glioma is often associated with cyst and calcification. These calcifications are well observed on CT as hyper-density, and on MR imaging seen as hyper-intensity on T1- and as hypo-intensity on T2*-weighted imaging. Mass effect in midbrain tectal glioma is frequently associated with hydrocephalus due to aqueduct obstruction. Brainstem glioma typically presents as an infiltrative diffuse lesion, seen as hypointensity on T1- and hyper-intensity on FLAIR/T2-weighted imaging, associated with diffuse enlargement of the brainstem (Fig. 2). Exophytic medullary glioma and midbrain tectal glioma are typically low-grade non-enhancing (although enhancement can be observed) lesions, whereas classical diffuse pontine gliomas are often high-grade lesions showing variable enhancement. Gliomas are mainly limited to the brainstem but may be associated with infiltration of adjacent brain regions, such as the cerebellum and the diencephalon.

Since histopathological sampling in the brainstem is at high risk, advanced MRI techniques (e.g. MRS, PWI, and DTI) can be useful to provide additional non-invasive information for the differentiation of brain tumours from other non-neoplastic lesions [19, 20]. In the absence of histopathological diagnosis, complementary investigations, such as whole body CT, F-DOPA-PET, and CSF analyses, might be useful to rule out other, non-neoplastic, disorders.

CNS Lymphoma

The vast majority of primary CNS lymphomas are supratentorial (typically involving frontal and parietal lobes, deep grey matter, and corpus callosum, with lesions clustering around the ventricles and the grey/white matter junction). CNS lymphoma presents with unique or multiple lesions on brain imaging, and are hypo/isointense on T1/T2/FLAIR imaging. Restricted diffusion, related to high proliferative activity of the lesion, is frequently observed in CNS lymphoma [21]. Surrounding oedema is classically absent or mild, and lesions are often associated with no or mild mass effect. Classically, strong and diffuse enhancement is observed on gadolinium-enhanced T1-weighted imaging, whereas ring-enhancing lesions with central necrosis can be observed in CNS lymphoma in immunocompromised patients. DWI often shows restricted diffusion, probably

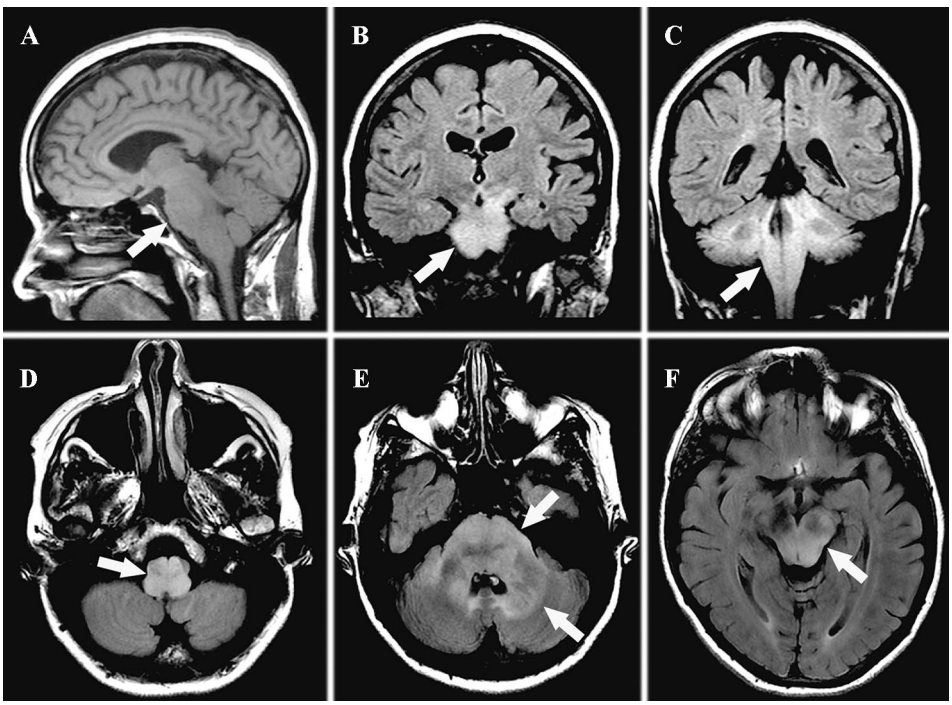

Fig. 2 MRI showing involvement of the entire brainstem on sagittal T1 sequence (**A**), and diffuse brainstem and cerebellar white matter infiltration (with left-sided predominance in the cerebellum and mesencephalon) on FLAIR imaging (**B** and **C**, coronal views; **D**–**F**, axial views)

because of high nuclear-to-cytoplasmic ratio and high cellular density of lymphoma. Signal changes and contrast enhancement often decrease or temporarily disappear after steroid treatment.

Haemangioblastoma

About 25% of haemangioblastomas are associated with von Hippel–Lindau disease (typically presenting with multiple lesions). Most of the lesions are observed in the posterior fossa, frequently involving the cerebellar hemispheres, whereas brainstem involvement (especially observed in the medulla oblongata) is rare.

On brain imaging, haemangioblastoma is typically observed as a cystic lesion associated with a mural nodule, or as a solid hyper-vascularised tumour. The solid portion of the haemangioblastoma is typically seen as a hypo-intensity on T1- and hyper-intensity on FLAIR/T2-weighted imaging, showing marked and homogeneous enhancement on gadolinium-injected T1-weighted imaging. T1 and T2 sequences can sometimes also show flow void, whereas T2*-weighted imaging may show susceptibility effect in the presence of blood breakdown products.

Ependymoma

About two-thirds of ependymoma occur in the posterior fossa, typically surrounding the fourth ventricle. Posterior fossa ependymoma are irregular in shape, often associated with cysts, calcifications, and haemorrhage [22]. Mass effect often leads to hydrocephalus. Tumour signal is typically heterogeneous, iso/hypo-intense on T1- and iso/hyper-intense on T2-weighted imaging. Cystic content is slightly hyper-intense to CSF signal on T1-weighted imaging, hyper-intense on T2-weighted imaging, and very hyper-intense to CSF on FLAIR. Calcifications and haemorrhage are typically hyperintense on T1- and hypointense on T2-weighted imaging, both showing hypointense susceptibility effect on T2*-weighted imaging. Mild-to-moderate heterogeneous enhancement is observed on gadolinium-injected T1-weighted imaging.

Metastasis

About 5% of brain CNS metastases occur in the brainstem, often associated with non-brainstem cerebral metastases. Metastatic lesions are typically observed as iso/hypo-intensity on T1-weighted imaging and iso/hyper-intensity on T2-weighted imaging and FLAIR, often associated with T2/FLAIR hyper-intense surrounding oedema. Some metastatic lesions (e.g. metastases from melanoma or haemorrhagic metastases) present with hyper-intensities on unenhanced T1-weighted imaging. Nodular or ring-like enhancement is typically observed in metastatic CNS lesions on gadolinium-injected T1-weighted imaging.

Histiocytosis

The histiocytoses are a heterogeneous group of disorders characterised by abnormal accumulation of histiocytes and cells of the mononuclear phagocytic system in various organs and tissues, rarely involving the CNS. In case of CNS involvement, the hypothalamic pituitary axis is the most frequent area involved. Other brain and cranial regions sometimes involved include the brainstem, cerebellar dentate nuclei, the basal ganglia, the paranasal sinuses, orbits, and meningeal involvement [23]. Almost half of the patients present with predominant brainstem (especially the pons) involvement. Brain lesions are often multiple, usually showing mixed hypo/hyper-intense signal on T2-weighted imaging. Associated oedema, mass effect, and (often homogeneous) contrast enhancement on gadolinium-injected T1-weighted imaging are frequently observed in these histiocytosis lesions.

Degenerative disorders

Multiple system atrophy

Multiple system atrophy (MSA) is an adult-onset, neurodegenerative disease characterised by progressive autonomic failure, Parkinsonism, cerebellar dysfunction, and pyramidal features in various combinations. One of the MRI abnormalities often observed in MSA is the so-called hot cross-bun sign, a cruciform pontine hyper-intensity on T2-weighted and FLAIR imaging resulting from atrophy of the pontine neurons and transverse pontocerebellar fibres preserving the pyramidal tract and pontine tegmentum, especially in MSA with predominant cerebellar dysfunction (MSA-C) (Fig. 3) [24]. T2*-weighted imaging has been shown to be superior to T2-weighted imaging in detecting the hot cross-bun sign, where it is seen as hyper-intensity [25]. However, the hot cross-bun sign, is not specific for MSA, and can be observed for instance in spinocerebellar ataxias [26]. Other MSA-related MRI changes include olivopontocerebellar atrophy (especially in MSA-C), putaminal atrophy, middle cerebellar peduncle T2/FLAIR hyper-intensities, and slit-like T2/FLAIR hyper-intense putaminal rim (and especially the discontinuity or irregular disruption of the rim), T2/FLAIR hypointensity at the dorsolateral putaminal margin, and hypointensities on iron-sensitive MRI sequences (T2*-weighted imaging and SWI) in the deep grey matter (especially in the posterior putamen) (Fig. 3) [24].

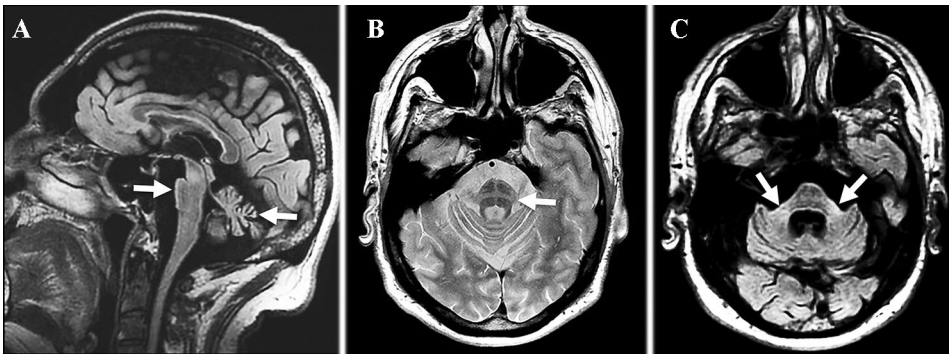

Fig. 3 MRI in a MSA patient showing pontocerebellar atrophy (**A**, sagittal T1-weighted imaging), hot cross-bun sign (**B**, axial T2-weighted imaging), and middle cerebellar peduncle hyper-intensities (**C**, axial FLAIR)

Progressive supra-nuclear palsy

Progressive supra-nuclear palsy (PSP) represents a group of related tauopathies. The brainstem variants PSP-predominant parkinsonism (PSP-P) and PSP-progressive gait freezing (PSP-PGF) show atrophy predominant in the midbrain, associated with reduced midbrain to pons ratio on sagittal images (resulting in a so-called hummingbird or penguin sign), reduction of the anteroposterior midline midbrain diameter on axial images (resulting in the so-called Micky mouse or morning glory sign) (Supplementary Fig. 5) [27].

Dentatorubral–pallidoluysian atrophy

Dentatorubral–pallidoluysian atrophy (DRPLA) is an autosomal dominant neurodegenerative disorder caused by CAG triplet expansion in *atrophin 1*. DRPLA-related MRI abnormalities include T2/FLAIR hyper-intensities in the cerebral (and to a lesser degree the cerebellar) white matter, thalamus, and brainstem, associated with atrophy of the brainstem and cerebellum (Supplementary Fig. 6) [28, 29]. DRPLA brainstem abnormalities are predominant in the pons and midbrain, and to a lesser degree the inferior olive.

Amyotrophic lateral sclerosis

Amyotrophic lateral sclerosis (ALS) is a progressive neurodegenerative disorder involving both upper and lower motor neurons. Due to involvement of the upper motor neurons (probably at least partly due to Wallerian degeneration), hyper-intensities involving the corticospinal tract (often well observed in the internal capsule because of the concentrated corticospinal fibers) can be observed on T2/FLAIR imaging (Supplementary Fig. 7) [30]. In the brainstem, bilateral symmetric hyper-intensities are often present in the areas corresponding to the corticospinal tracts (Supplementary Fig. 7). However, this MRI abnormality yields relatively low sensitivity and specificity for ALS. In ALS, associated bilateral precentral cortical hypo-intensities can sometimes be seen on T2*-weighted imaging and SWI, thought to be related to iron accumulation within microglia in the motor cortex.

Demyelinating inflammatory lesions

Multiple sclerosis

Multiple sclerosis (MS) lesions appear typically as T2 and FLAIR hyper-intensities most commonly involving in the periventricular white matter (often presenting as ovoid or linear lesions), corpus callosum (especially the inferior part), and the posterior fossa, and sometimes also the cerebral cortex. In acute MS lesions, gadolinium enhancement is typically observed and restricted diffusion can sometimes be seen on diffusion-weighted imaging. Brainstem lesions are important since the presence of these lesions increases both the risk of conversion to MS in patients with clinically isolated syndromes and the risk of long-term disability in MS patients [31–34]. The pons is the most frequently involved brainstem substructure, followed by the midbrain and the medulla oblongata (Supplementary Fig. 8). The middle cerebellar peduncles are more frequently involved than the cerebellar hemispheres.

Linear hyper-intensities in the intra-axial pontine portion of the trigeminal root can be observed (especially when using high-field strength MRI) in MS patients, including patients without facial sensory symptoms (Supplementary Fig. 8) [35].

Solitary sclerosis

Solitary sclerosis (SS) is an isolated demyelinating CNS lesion located typically in the cervical spinal cord or the cervico-medullary junction (and sometimes in the thoracic spinal cord or the brainstem) [36]. Typical SS lesions are spinal cord lesions less than three vertebral segments in length showing increased signal on T2-weighted imaging

and absence of contrast enhancement. Some SS patients will develop new lesions, and fulfil MS criteria.

Neuromyelitis optica spectrum disorder and myelin-oligodendrocyte-glycoprotein-antibody-associated disorder

Neuromyelitis optica spectrum disorder (NMOSD), an inflammatory disease of the CNS characterised by severe attacks of optic neuritis and longitudinally extensive transverse myelitis, was initially thought to show no or only discrete brain MRI abnormalities. However, recent studies systematically analysing brain lesions in NMOSD have shown that these lesions are very frequent with radiological abnormalities sometimes characteristic for NMOSD. Non-specific small dots and patches of T2/FLAIR hyper-intensity in subcortical and deep white matter are the most common findings in NMOSD. Lesions tend to be more diffuse, heterogeneous, cystic, and with blurred margins than observed in MS. NMOSD lesions are frequently located in areas associated with high AQP4 expression, i.e. peri-ependymal areas surrounding the ventricular system. Therefore, in the brainstem, mesencephalic lesions surrounding the cerebral aqueduct and dorsal brainstem lesions adjacent to the fourth ventricle (including the area postrema and the nucleus tracts solitaries) are frequently observed in NMOSD [37, 38]. In addition, lesions involving the brainstem corticospinal tracts, as well as the supra-tentorial corticospinal tracts, have been reported. Brainstem lesion have been observed in up to half of the NMOSD patients. Gadolinium enhancement can be observed in a minority of patients, showing poorly marginated, subtle, and multiple patchy pattern (leading to a so-called "cloud-like" enhancement), or linear enhancement of the ependymal surface of the ventricles. In myelin-oligodendrocyte-glycoprotein-antibody-associated disorder (MOGAD), similar brainstem lesions can be observed as in NMOSD [39]. In both MOGAD and NMOSD patients with brainstem or cerebellar symptoms, medullar and pontine involvement was observed more frequently than midbrain lesions on MRI (with medullar lesions more frequent in NMOSD and pontine lesions more frequent in MOGAD) [39].

Acute disseminated encephalomyelitis

Acute disseminated encephalomyelitis (ADEM) is a monophasic post-infection or post-vaccination disorder with radiological features partially overlapping with MS. The most common MRI finding is the presence of multiple bilateral T2/FLAIR supra-tentorial white matter lesions, often accompanied by lesions in the thalamus, the basal ganglia, the brainstem, the cerebellum or the spinal cord [40]. Lesions vary from multifocal punctate to large flocculent or pseudo-tumoural lesions. Compared to MS, corpus callosum and periventricular lesions are less frequent and thalamic and basal ganglia lesions far more frequent in ADEM. Although variable, gadolinium-enhanced T1-weighted imaging typically shows punctate, ring, or incomplete ring enhancement of all (or nearly all) lesions.

Non-demyelinating inflammatory lesions

Neuro-Behçet's disease

Behçet's disease is a relapsing inflammatory multisystem disease, often also involving the CNS (i.e. Neuro-Behçet's disease, NBD). The predilection site of characteristic NBD lesions is the brainstem, usually involving the pons and often extending upwards to the midbrain, the diencephalon, and the basal ganglia (Fig. 4) [41]. Acute and subacute lesions are hyper-intense on T2/FLAIR, often showing gadolinium enhancement on contrast-enhanced T1-weighted imaging. In the chronic phase, lesions tend to decrease in size or resolve completely. In NBD, multiple small periventricular white matter lesions are also often observed.

Chronic lymphocytic inflammation with pontine perivascular enhancement responsive to steroids

Chronic lymphocytic inflammation with pontine perivascular enhancement responsive to steroids (CLIPPERS) is a recently described CNS inflammatory syndrome with characteristic lesions consisting of multiple small, punctuate and curvilinear gadolinium-enhancing lesions involving (or "peppering") the brainstem (especially involving the pons and brachium pontis, and less often the midbrain and medulla) and the cerebellar white matter (Supplementary Fig. 9) [42, 43]. Associated lesions in the cervical spinal cord, basal ganglia, thalamus, and cerebral white matter are

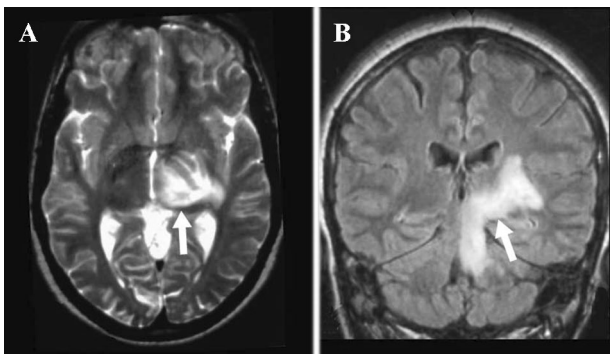

Fig. 4 Axial T2-weighted (**A**) and coronal FLAIR (**B**) imaging showing a left-sided NBD brainstem lesion extending into the diencephalon and the deep grey matter

relatively frequent. Contrast-enhancing lesions typically improve dramatically, at least transitory, after corticoid treatment. Contrast-enhancing lesions are usually associated with mild to moderate hyper-intensity on T2/FLAIR, not extending beyond the boundaries of the contrast enhancement (i.e. suggestive of absence of vasogenic oedema).

Other non-demyelinating inflammatory diseases

In other non-demyelinating inflammatory diseases (e.g. Sjögren syndrome, lupus erythematosus, sarcoidosis, etc.) brainstem lesions can be sometimes observed, often associated with periventricular white matter lesions. Both enhancing and non-enhancing lesions have been described in these disorders, sometimes associated with leptomeningeal involvement. Although brainstem lesions can be observed, the brainstem (unlike NBD) is not a predilection site of these non-demyelinating inflammatory diseases.

Metabolic diseases

Osmotic demyelination syndrome

The osmotic demyelinating syndrome (ODS), formerly called central pontine myelinolysis (because of the frequent pontine involvement) or extrapontine myelinolysis (when lesions other than pontine are present), can be observed with any kind of osmotic gradient changes (e.g. rapid iatrogenic correction of hyponatremia in patients with alcoholism, chronic liver disease, or malnutrition).

Pontine ODS typically involves the posterior pontine, transverse pontocerebellar, and pontine midline structures [44, 45]. When progressing, hyper-intensities tend to spread out anteriorly by encircling and respecting pyramidal tracts giving a trident-shaped aspect (Fig. 5). In severe pontine ODS, a large homogeneous pontine lesion can be observed. A wing- or eagle-like lesion can be seen at intermediate stages of ODS (Fig. 5).

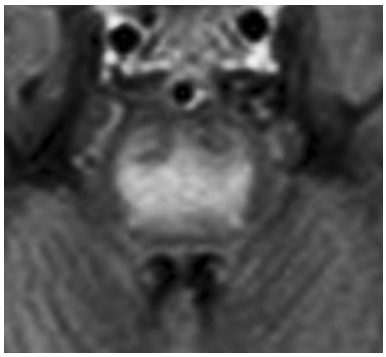

Fig. 5 Axial FLAIR showing a central pontine hyperintensity encircling and respecting the pyramidal tracts giving the ODS lesion a wing- or eagle-like aspect

When present, the most frequent extrapontine localisations of ODS include (in descending order of frequency) the cerebellum, the lateral geniculate body, the external and extreme capsule, the hippocampus, the putamen, the cerebral cortex/sub-cortex, the thalamus, and the caudate nucleus.

ODS lesions are T2/FLAIR hyper-intense and T1 hypo-intense in the acute phase, and often resolve after the acute phase. Lesions may occur within a certain delay after the onset of clinical symptoms or may even be seen in absence of clinical abnormalities. Hemorrhage and contrast enhancement are rare. Lesions sometimes occur with a certain delay after the onset of clinical symptoms. Increased DWI signal and heterogeneous signal changes on ADC map often accompany the changes on T1- and T2-weighted imaging [46].

Wernicke encephalopathy

Wernicke encephalopathy (WE), related to vitamin B1 deficiency, typically affects the periaqueductal mesencephalic grey matter, the mammillary bodies, the medial thalamus, the hypothalamus, cranial nerve nuclei (especially the medial vestibular nuclei), and the perirolandic regions (Supplementary Fig. 10) [47]. Lesions are usually symmetrical and best seen on T2/FLAIR sequences as hyper-intensity. Less frequently involved brain areas in WE include the cerebellar dentate nuclei, the cerebellar peduncles, the vermis, the corpus callosum, and the caudate nucleus. Involvement of the red nuclei and substantia nigra in the midbrain or diffuse brainstem lesions can sometimes be observed [48]. In the acute phase of WE, enhancement (especially in alcoholic patients) and/or restricted diffusion can sometimes be observed. Haemorrhagic lesions have been reported in very severe cases.

Hepatic encephalopathy

Signal changes observed in hepatic encephalopathy (HE) include hyper-intensities on T1-weighted imaging (probably related to the accumulation of manganese) predominant in the basal ganglia (especially in the medial segment of the globus pallidus) and sometimes also observed in the anterior part of the midbrain (involving especially the substantia nigra), increased T2 and FLAIR signal in the cerebral and brainstem corticospinal tract similar to ALS (Supplementary Fig. 11) [49]. MRI abnormalities are often reversible with improved liver function.

Posterior reversible encephalopathy syndrome

In posterior reversible encephalopathy syndrome (PRES), MRI typically shows bilateral T2/FLAIR white matter hyper-intensities in the occipital and posterior parietal lobes, frequently associated with involvement of watershed areas between middle and posterior cerebral arteries. When studied systematically, associated involvement of other brain regions (including the frontal and temporal white matter, basal ganglia, thalamus, corpus callosum, cerebral cortex, cerebellum, and brainstem) is frequently observed.

MRI characteristics are indicative for vasogenic oedema (hyper-intense signal on FLAIR, T2-weighted imaging and ADC map, normal or slightly increased signal on DWI, and iso- to hypointense signal on T1-weighted images). ADC values seem to be more sensitive to show signal changes than findings on conventional T2 and FLAIR sequences.

PRES-related infarction (due to decreased cerebral blood flow in areas of massive oedema and elevated tissue perfusion pressure), haemorrhage (especially when associated with hypertension), and/or gadolinium enhancement are sometimes observed. In case of infarction, the affected regions show highly increased signal on DWI, and pseudo-normalised or decreased signal on ADC map. In uncomplicated patients, regression (at least partially) of the radiological abnormalities is typically observed after discontinuation of the offending drug and the treatment of elevated blood pressure.

In a large review of the literature, brainstem involvement was observed in more than 20% of patients, with the pons as the most frequently involved brainstem substructure, followed by the midbrain and the medulla [50]. In most of the reported PRES cases with brainstem involvement, hyper-intensities were diffuse and often associated with severe brainstem swelling (Fig. 6).

Leigh syndrome

Leigh syndrome (LS) is a neurodegenerative disease with variable symptoms typically manifesting in infancy or early childhood, caused by mitochondrial dysfunction from a hereditary genetic defect and bilateral symmetrical CNS lesions, typically involving the basal ganglia (especially the putamen) and the brainstem [51, 52]. On MRI, brainstem involvement is observed in about half of the cases, frequently involving the substantia nigra, nucleus ruber, and medulla oblongata. Other brain areas, such as the thalamus, cerebellum (especially the cerebellar dentate nuclei), and spinal cord, are sometimes involved in LS. Typical LS lesions are symmetrical and seen as hyper-intensity on T2-weighted and FLAIR imaging, as

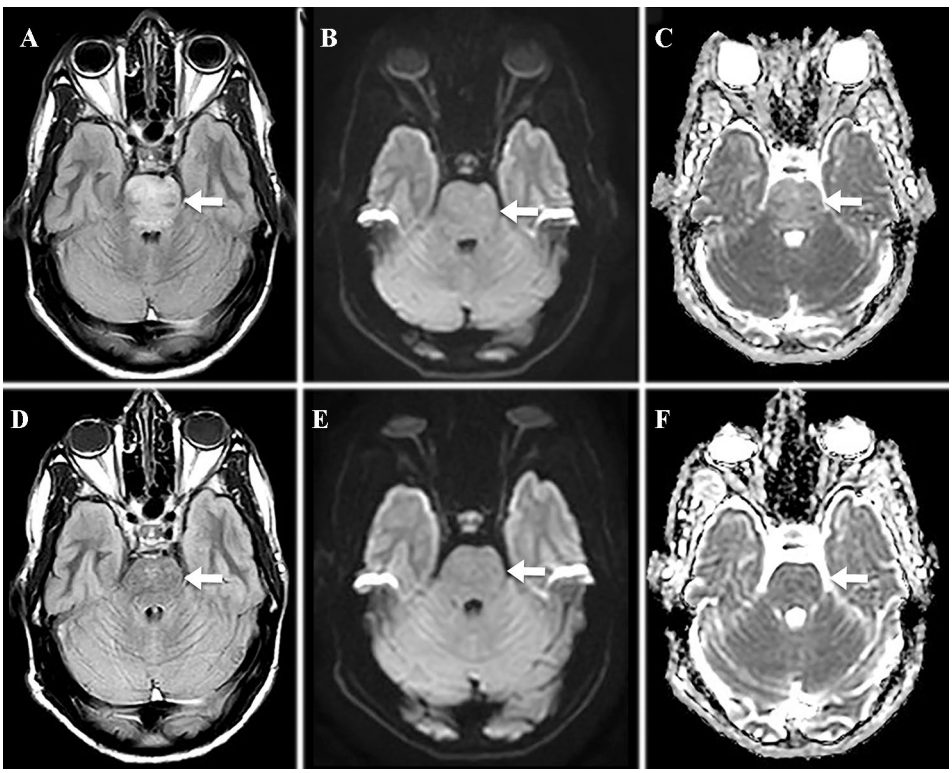

Fig. 6 MRI in a PRES patient showing diffuse pontine hyper-intensities on FLAIR (**A**) and ADC map (**C**), isointense on DWI (**B**). After treatment of hypertension and renal insufficiency, radiological abnormalities nearly normalised (slight hyper-intensity persisting on FLAIR) on MRI two months later (**D**, FLAIR; **E**, DWI, **F**, ADC map)

hypo-intensity on T1-weighted imaging, and sometimes showing restricted diffusion in the acute phase.

Other brain MRI changes (including leukoencephalopathy, stroke-like lesions, cerebral and cerebellar atrophy) frequently associated with other mitochondrial syndromes can be sometimes observed in LS.

In LS, like in other mitochondrial diseases, proton magnetic resonance spectroscopy typically shows a lactate peak.

Wilson disease

Neurological symptoms in Wilson disease (WD), a rare autosomal recessive disorder, are caused by nervous tissue damage that is primarily a consequence of extrahepatic (i.e. brain) copper toxicity.

Typical MRI findings in WD are symmetric T2/FLAIR hyper-intensities (and corresponding T1 hypo-intensities) in the deep grey matter (with the putamen as most frequently involved structure with a distinctive lateral rim of high-signal intensity, followed by the caudate nucleus and the ventral thalamus) and the brainstem [53–55]. Sometimes, signal is decreased on T2-weighted and increased on T1-weighted imaging due to the paramagnetic effect of copper. The most frequent brainstem WD lesions concern the white matter (predominant in the tectal region) and are observed in the pons, followed by the midbrain and the medulla [55]. The intensity of the superior colliculus (normally equivalent to the signal of the cerebral white matter) is sometimes observed decreased in WD. Signal changes on T2-weighted images of the axial midbrain section often result in a so-called "face of giant panda" (resulting from white matter midbrain hyper-intensities sparing the red nucleus, associated with WB-related superior colliculus and physiological substantia nigra hypo-intensities). Other brain areas sometimes involved in WD include the cerebellar peduncles, the cerebellum, and the supra-tentorial white matter (often asymmetric, with frontal predominance). In the early phase after onset of neurological symptoms, some patients present with lesions showing restricted diffusion on diffusion-weighted imaging. In end stage WD, lesions often become hypo-intense on FLAIR. MRI lesions are partly reversible upon anti-copper treatment. Atrophy (sometimes after an initial phase of oedema and swelling) of the involved brain structures is typically seen in late stage WD. In case of severe irreversible tissue damage, lesions may progress to necrosis leading to cavitary lesion (especially in the putamen). Contrast enhancement is typically absent.

Paraneoplastic/autoimmune encephalitis

If present, the most frequent brain MRI abnormality observed in autoimmune or paraneoplastic encephalitis is limbic hyper-intensity on T2/FLAIR and/or DWI (in case of so-called limbic encephalitis). However, multiple extra-limbic brain regions (including the brainstem) have been reported to show MRI signal changes in autoimmune/paraneoplastic encephalitis [56]. When present, brainstem lesions are usually diffuse, hyper-intense on T2-weighted imaging and FLAIR, symmetric or asymmetric, and sometimes associated with restricted diffusion on diffusion-weighted imaging and contrast enhancement on gadolinium-injected T1-weighted imaging [57]. Antibodies reported to be associated with brainstem encephalitis and MRI signal changes include anti-Ma2, -Ri, and -GQ1B antibodies.

Inherited leukoencephalopathies

Genetic leukoencephalopathies (often referred to as leukodystrophies) are a heterogeneous group of disorders with distinct pathologic mechanisms, but sharing the presence of diffuse white matter hyper-intensities on T2/FLAIR [58]. Some specific MRI findings, including the presence and subtype of brainstem involvement, can help to distinguish these disorders from each other [59]. For instance, brainstem involvement is frequently observed in leukoencephalopathy with brainstem and spinal cord involvement and lactate elevation, autosomal dominant adult-onset demyelinating leukodystrophy, adult poly-glucosan body disease, and Alexandre disease. Brainstem signal changes observed in genetic leukoencephalpathies include T2/FLAIR hyper-intensities involving the corticospinal tract, the medial lemniscus, the core of the pons, and the area surrounding the aqueduct and the fourth ventricle. Associated brainstem atrophy can be observed in several of these disorders. Enhancement is generally absent, although in some disorders (e.g. adrenoleukodystrophy and Alexandre disease), gadolinium enhancement can sometimes be observed.

Wallerian degeneration

After an acute brain lesion (e.g. infarction, acute MS lesion), a process of Wallerian degeneration (a progressive anterograde disintegration after injury to the proximal axon or cell body) can be observed involving remote brain areas including the brainstem. Signals on T1- and T2-weighted imaging depend on the timing/stage of Wallerian degeneration, with, in the acute stage no signal changes, increased T1 and decreased T2 signal in the subacute stage, decreased T1 and increased signal in the chronic stage, and atrophy and possible normalisation of the signal in the late chronic stage. Brainstem Wallerian degeneration typically involves the corticospinal tract (e.g. after supra-tentorial infarction), pontocerebellar tract, or the dentate-rubro-olivary pathway (Supplementary Fig. 12) [60]. Sometimes restricted

diffusion can be observed in the early phase of Wallerian degeneration.

Hypertrophic olivary degeneration

Hypertrophic olivary degeneration (HOD) is related to trans-synaptic degeneration caused by the loss of afferent signals into the inferior olivary nucleus in the medulla (similar to the process of Wallerian degeneration). On MRI, the inferior olivary nucleus is enlarged and shows hyper-intensities on T2/FLAIR imaging (Fig. 7 and Supplementary Fig. 13) [61]. HOD usually develops following a lesion involving the dentato-rubro-olivary pathway within the so-called triangle of Guillain and Mollaret. HOD can be unilateral or bilateral, with known or unknown cause. Cerebrovascular disease (e.g. haemorrhage, infarction) is the most frequent cause of HOD, followed by tumour, priori posterior fossa surgery, and MS. In secondary HOD, MRI also shows the primary lesions involving the dentato-rubro-olivary pathway causing HOD. Enlargement and hyper-intensity of the inferior olivary nucleus can increase or decrease over time.

Infectious diseases

Infectious rhombencephalitis

The two most frequent infectious agents causing infectious rhombencephalitis (IRE) are *Listeria monocytogenes* and *Mycobacterium tuberculosis*. IRE related to other infectious agents include enterovirus 71, herpes simplex virus 1 and 2, Epstein–Barr virus, human herpes virus 6, and *Mycoplasma pneumonia*.

Although MRI signal depends on the infectious agent involved and the disease stage, IRE encephalitis often shows increased T2/FLAIR signal (often adjacent to the areas of leptomeningeal enhancement) and mass effect, in later stages appearing as (micro)abscesses showing solid or ring-like contrast enhancement [62]. Associated leptomeningeal involvement is classically observed, seen as FLAIR hyper-intensity and enhancement on gadolinium-injected T1-weighted imaging (and sometimes together with cranial nerve enhancement). High T1 and low T2 signal within the solid portion of the lesions are suggestive of *Mycoplasma pneumonia* infection. Focal arterial stenosis (seen on MRA or CTA) and infarction (best seen on diffusion-weighted imaging) is suggestive of *Mycobacterium tuberculosis* infection.

Progressive multifocal leukoencephalopathy

Progressive multifocal leukoencephalopathy (PML) is a severe infection caused by the polyomavirus JC involving the CNS, most often in immunocompromised patients (e.g. HIV patients and MS patients treated with natalizumab).

Typical PML lesions are hyper-intense on T2/FLAIR and hypo-intense on T1 lesions, uni- or multifocal, and most often involve cerebral (and sometimes cerebellar) subcortical white matter respecting the deep grey matter and the cortex in the absence of mass effect. Although usually absent, faint contrast enhancement can be observed at the periphery of the lesions. Patients surviving PML typically show severe atrophy of the involved brain structures. Several cases of isolated brainstem PML at disease onset have been reported [63]. Half of the reported cases involved the pons. With the exception of one patient showing slight peripheral enhancement of the midbrain lesion after gadolinium injection, reported cases with brainstem PML lacked enhancement on MRI.

The use of natalizumab for MS is associated with an increased risk for PML. MRI features differentiating PML from MS include DWI hyper-intensity, U-fibre involvement, non-periventricular localisation, punctate T2 lesions in the vicinity (also described as "milky way appearance") or further away of the main PML lesion, cortical grey matter and juxta-cortical white matter lesion, ill-defined and mixed

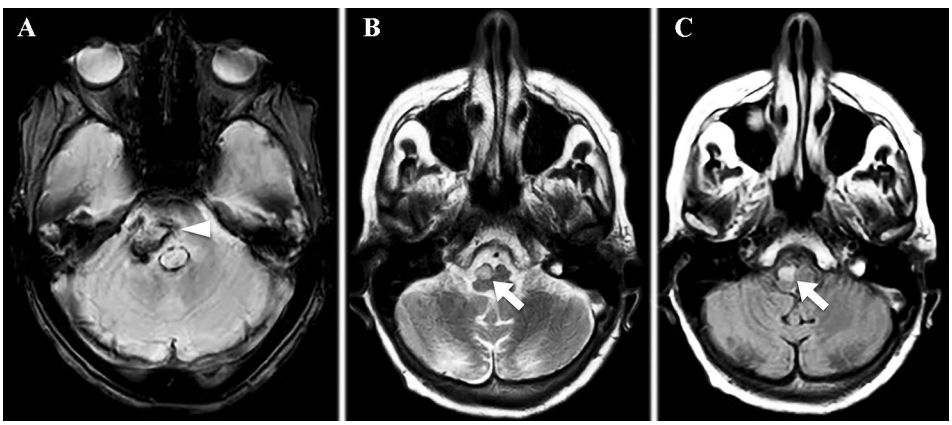

Fig. 7 MRI in a patient with a recent right-sided hemorrhage (**A**, T2*-weighted imaging) showing unilateral HOD (**B**, T2-weighted imaging; **C**, FLAIR)

borders (compared to sharp borders), lesions size > 3 cm, and contrast enhancement [64, 65].

Trauma

Diffuse axonal injury (DAI), related to severe head trauma, typically involves the corpus callosum, the midbrain, and the lobar white matter (especially involving the grey–white matter junction). DAI is best seen on diffusion-weighted imaging and FLAIR sequences as multifocal hyper-intensities, frequently associated with CMB. On ADC map, lesions may be hypo-intense, indicating cytotoxic oedema. DAI is often associated with other radiological manifestations of head trauma, including epidural, subdural, subarachnoid, or intraventricular hemorrhage, contusion and/or cervical artery dissection.

About 20% of DAI involve the brainstem (Supplementary Fig. 14) [66]. Large dorsal pontine DAI lesions are related to poor outcome and decreased consciousness at hospital discharge.

Supplementary Information The online version contains supplementary material available at https://doi.org/10.1007/s13760-022-01943-y.

Acknowledgements We would like to thank Dr. Sarah Kabani (Service de Biostatistique, Epidémiologie Clinique, Santé Publique et Innovation en Méthodologie (BESPIM), CHU de Nîmes, 4 Rue du Professeur Debré, 30029 Nîmes Cedex 09) for proofreading our manuscript.

Declarations

Conflict of interest The authors declare that they have no conflict of interest.

Ethical statement The subject has given her informed consent to report data given. The manuscript was approved by the institute's committee on human research.

References

1. Tatu L, Moulin T, Bogousslavsky J, Duvernoy H (1996) Arterial territories of human brain: Brainstem and cerebellum. Neurology 47(5):1125–1135
2. Connell L, Koerte IK, Laubender RP, Morhard D, Linn J, Becker HC et al (2012) Hyperdense basilar artery sign—a reliable sign of basilar artery occlusion. Neuroradiology 54(4):321–327
3. Ernst M, Romero JM, Buhk J-H, Cheng B, Herrmann J, Fiehler J, et al. Sensitivity of Hyperdense Basilar Artery Sign on Non-Enhanced Computed Tomography. Hendrikse J, editor. PLoS ONE. 2015 Oct 19;10(10):e0141096.
4. Sylaja PN, Coutts SB, Krol A, Hill MD, Demchuk AM (2008) When to Expect Negative Diffusion-Weighted Images in Stroke and Transient Ischemic Attack. Stroke 39(6):1898–1900
5. Chen X, Wang J, Shan Y, Cai W, Liu S, Hu M et al (2019) Cerebral small vessel disease: neuroimaging markers and clinical implication. J Neurol 266(10):2347–2362
6. Hakky MM, Erbay KD, Brewer E, Midle JB, French R, Erbay SH (2013) T2 Hyperintensity of medial lemniscus: higher threshold application to ROI measurements is more accurate in predicting small vessel disease. J Neuroimaging 23(3):345–351
7. Erbay SH, Brewer E, French R, Midle JB, Zou KH, Lee GM et al (2012) T2 Hyperintensity of medial lemniscus is an indicator of small-vessel disease. Am J Roentgenol 199(1):163–168
8. Fakan B, Reisz Z, Zadori D, Vecsei L, Klivenyi P, Szalardy L (2020) Predictors of localization, outcome, and etiology of spontaneous intracerebral hemorrhages: focus on cerebral amyloid angiopathy. J Neural Transm 127(6):963–972
9. Aguilar MI, Brott TG (2011) Update in Intracerebral Hemorrhage. The Neurohospitalist 1(3):148–159
10. Flemming KD, Link MJ, Christianson TJH, Brown RD (2012) Prospective hemorrhage risk of intracerebral cavernous malformations. Neurology 78(9):632–636
11. Kashefiolasl S, Bruder M, Brawanski N, Herrmann E, Seifert V, Tritt S et al (2018) A benchmark approach to hemorrhage risk management of cavernous malformations. Neurology 90(10):e856–e863
12. Salman RA-S, Hall JM, Horne MA, Moultrie F, Josephson CB, Bhattacharya JJ, et al (2012) Untreated clinical course of cerebral cavernous malformations: a prospective, population-based cohort study. Lancet Neurol 11(3):217–24
13. Hou K, Li G, Qu L, Liu H, Xu K, Yu J (2020) Intracranial dural arteriovenous fistulas with brainstem engorgement: an underrecognized entity in diagnosis and treatment. Front Neurol 11:526550
14. Grigoryan G, Sitnikov A, Grigoryan Y (2020) Hemifacial spasm caused by the brainstem developmental venous anomaly: a case report and review of the literature. Surg Neurol Int 6(11):141
15. Rudie JD, Rauschecker AM, Nabavizadeh SA, Mohan S (2018) Neuroimaging of dilated perivascular spaces: from benign and pathologic causes to mimics: perivascular spaces. J Neuroimaging 28(2):139–149
16. Kwee RM, Kwee TC (2007) Virchow-robin spaces at MR imaging. Radiographics 27(4):1071–1086
17. Wardlaw JM, Smith C, Dichgans M (2019) Small vessel disease: mechanisms and clinical implications. Lancet Neurol 18(7):684–696
18. Reyes-Botero G, Mokhtari K, Martin-Duverneuil N, Delattre J, Laigle-Donadey F (2012) Adult brainstem gliomas. Oncologist 17(3):388–397
19. Villanueva-Meyer JE, Mabray MC, Cha S (2017) Current clinical brain tumor imaging. Neurosurgery 81(3):397–415
20. Fink JR, Muzi M, Peck M, Krohn KA (2015) Multimodality brain tumor imaging: MR imaging, PET, and PET/MR imaging. J Nucl Med 56(10):1554–1561
21. Schob S, Meyer J, Gawlitza M, Frydrychowicz C, Müller W, Preuss M, et al (2016) Diffusion-Weighted MRI reflects proliferative activity in primary CNS lymphoma. Coles JA, editor. PLoS ONE 11(8):e0161386.
22. Yuh EL, Barkovich AJ, Gupta N (2009) Imaging of ependymomas: MRI and CT. Childs Nerv Syst 25(10):1203
23. Luna LP, Drier A, Aygun N, Mokhtari K, Hoang-Xuan K, Galanaud D et al (2021) MRI features of intra-axial histiocytic brain mass lesions. Clin Radiol 76(2):159.e19-159.e28
24. Kim H-J, Jeon B, Fung VSC (2017) Role of magnetic resonance imaging in the diagnosis of multiple system atrophy. Mov Disord Clin Pract 4(1):12–20
25. Deguchi K, Ikeda K, Kume K, Takata T, Kokudo Y, Kamada M et al (2015) Significance of the hot-cross bun sign on T2*-weighted MRI for the diagnosis of multiple system atrophy. J Neurol 262(6):1433–1439
26. Mascalchi M, Vella A (2018) Neuroimaging Applications in Chronic Ataxias. In: International Review of Neurobiology

[Internet]. Elsevier [cited 2021 Feb 19]. p. 109–62. Available from: https://linkinghub.elsevier.com/retrieve/pii/S0074774218301119
27. Whitwell JL, Höglinger GU, Antonini A, Bordelon Y, Boxer AL, Colosimo C et al (2017) Radiological biomarkers for diagnosis in PSP: Where are we and where do we need to be? Neuroimaging Biomarkers for Diagnosis in PSP. Mov Disord 32(7):955–971
28. Sugiyama A, Sato N, Nakata Y, Kimura Y, Enokizono M, Maekawa T et al (2018) Clinical and magnetic resonance imaging features of elderly onset dentatorubral-pallidoluysian atrophy. J Neurol 265(2):322–329
29. Sugiyama A, Sato N, Kimura Y, Fujii H, Shigemoto Y, Suzuki F, et al (2020) The cerebellar white matter lesions in dentatorubral-pallidoluysian atrophy. J Neurol Sci 416:117040
30. Fabes J, Matthews L, Filippini N, Talbot K, Jenkinson M, Turner MR (2017) Quantitative FLAIR MRI in Amyotrophic Lateral Sclerosis. Acad Radiol 24(10):1187–1194
31. Sastre-Garriga J, Tintoré M, Nos C, Tur C, Río J, Téllez N et al (2010) Clinical features of CIS of the brainstem/cerebellum of the kind seen in MS. J Neurol 257(5):742–746
32. Tintore M, Rovira A, Arrambide G, Mitjana R, Rio J, Auger C et al (2010) Brainstem lesions in clinically isolated syndromes. Neurology 75(21):1933–1938
33. Minneboo A, Barkhof F, Polman CH, Uitdehaag BMJ, Knol DL, Castelijns JA (2004) Infratentorial Lesions Predict Long-term Disability in Patients With Initial Findings Suggestive of Multiple Sclerosis. Arch Neurol 61(2):217
34. Nakashima I, Fujihara K, Okita N, Takase S, Itoyama Y (1999) Clinical and MRI study of brain stem and cerebellar involvement in Japanese patients with multiple sclerosis. J Neurol Neurosurg Psychiatry 67(2):153–157
35. Nakashima I, Fujihara K, Kimpara T, Okita N, Takase S, Itoyama Y (2001) Linear pontine trigeminal root lesions in multiple sclerosis: clinical and magnetic resonance imaging studies in 5 cases. Arch Neurol [Internet]. 2001 Jan 1 [cited 2021 Feb 19];58(1). Available from: http://archneur.jamanetwork.com/article.aspx?doi=https://doi.org/10.1001/archneur.58.1.101
36. Keegan BM, Kaufmann TJ, Weinshenker BG, Kantarci OH, Schmalstieg WF, Paz Soldan MM et al (2016) Progressive solitary sclerosis: Gradual motor impairment from a single CNS demyelinating lesion. Neurology 87(16):1713–1719
37. Chan KH (2011) Brain involvement in neuromyelitis optica spectrum disorders. Arch Neurol 68(11):1432
38. Kim HJ, Paul F, Lana-Peixoto MA, Tenembaum S, Asgari N, Palace J et al (2015) MRI characteristics of neuromyelitis optica spectrum disorder: an international update. Neurology 84(11):1165–1173
39. Banks SA, Morris PP, Chen JJ, Pittock SJ, Sechi E, Kunchok A et al (2021) Brainstem and cerebellar involvement in MOG-IgG-associated disorder versus aquaporin-4-IgG and MS. J Neurol Neurosurg Psychiatry 92(4):384–390
40. Koelman DLH, Mateen FJ (2015) Acute disseminated encephalomyelitis: current controversies in diagnosis and outcome. J Neurol 262(9):2013–2024
41. Kalra S, Silman A, Akman-Demir G, Bohlega S, Borhani-Haghighi A, Constantinescu CS et al (2014) Diagnosis and management of Neuro-Behçet's disease: international consensus recommendations. J Neurol 261(9):1662–1676
42. Simon NG, Parratt JD, Barnett MH, Buckland ME, Gupta R, Hayes MW et al (2012) Expanding the clinical, radiological and neuropathological phenotype of chronic lymphocytic inflammation with pontine perivascular enhancement responsive to steroids (CLIPPERS). J Neurol Neurosurg Psychiatry 83(1):15–22
43. Taieb G, Duflos C, Renard D, Audoin B, Kaphan E, Pelletier J et al (2012) Long-term Outcomes of CLIPPERS (Chronic Lymphocytic Inflammation With Pontine Perivascular Enhancement Responsive to Steroids) in a Consecutive Series of 12 Patients. Arch Neurol [Internet]. 69(7). Available from: http://archneur.jamanetwork.com/article.aspx?doi=https://doi.org/10.1001/archneurol.2012.122
44. Martin RJ (2004) Central pontine and extrapontine myelinolysis: the osmotic demyelination syndromes. J Neurol Neurosurg Psychiatry. 2004 75(suppl_3):iii22–8
45. Kallakatta RN, Radhakrishnan A, Fayaz RK, Unnikrishnan JP, Kesavadas C, Sarma SP (2011) Clinical and functional outcome and factors predicting prognosis in osmotic demyelination syndrome (central pontine and/or extrapontine myelinolysis) in 25 patients. J Neurol Neurosurg Psychiatry 82(3):326–331
46. Ruzek KA, Campeau NG, Miller GM (2004) Early diagnosis of central pontine myelinolysis with diffusion-weighted imaging. AJNR Am J Neuroradiol 25(2):210–213
47. Manzo G, De Gennaro A, Cozzolino A, Serino A, Fenza G, Manto A (2014) MR imaging findings in alcoholic and nonalcoholic acute Wernicke's encephalopathy: a review. Biomed Res Int 2014:1–12
48. Nardone R, Venturi A, Golaszewski S, Caleri F, Tezzon F, Ladurner G (2010) MR atypical wernicke encephalopathy showing extensive brain stem and diencephalic involvement. J Neuroimaging 20(2):204–207
49. Rovira A, Alonso J, Córdoba J (2008) MR imaging findings in hepatic encephalopathy. AJNR Am J Neuroradiol 29(9):1612–1621
50. Li K, Yang Y, Guo D, Sun D, Li C (2020) Clinical and MRI features of posterior reversible encephalopathy syndrome with atypical regions: a descriptive study with a large sample size. Front Neurol 24(11):194
51. Bonfante E, Koenig MK, Adejumo RB, Perinjelil V, Riascos RF (2016) The neuroimaging of Leigh syndrome: case series and review of the literature. Pediatr Radiol 46(4):443–451
52. Baertling F, Rodenburg RJ, Schaper J, Smeitink JA, Koopman WJH, Mayatepek E et al (2014) A guide to diagnosis and treatment of Leigh syndrome. J Neurol Neurosurg Psychiatry 85(3):257–265
53. Salari M, Fayyazi E, Mirmosayyeb O (2018) Magnetic resonance imaging findings in diagnosis and prognosis of Wilson disease. J Res Med Sci 23(1):23
54. Dusek P, Litwin T, Członkowska A (2019) Neurologic impairment in Wilson disease. Ann Transl Med 7(S2):S64–S64
55. Hitoshi S, Iwata M, Yoshikawa K (1991) Mid-brain pathology of Wilson's disease: MRI analysis of three cases. J Neurol Neurosurg Psychiatry 54(7):624–626
56. Demaerel P, Van Dessel W, Van Paesschen W, Vandenberghe R, Van Laere K, Linn J (2011) Autoimmune-mediated encephalitis. Neuroradiology 53(11):837–851
57. Michev A, Musso P, Foiadelli T, Trabatti C, Lozza A, Franciotta D et al (2019) Bickerstaff Brainstem Encephalitis and overlapping Guillain-Barré syndrome in children: report of two cases and review of the literature. Eur J Paediatr Neurol 23(1):43–52
58. Köhler W, Curiel J, Vanderver A (2018) Adulthood leukodystrophies. Nat Rev Neurol 14(2):94–105
59. Ayrignac X, Boutiere C, Carra-dalliere C, Labauge P (2016) Posterior fossa involvement in the diagnosis of adult-onset inherited leukoencephalopathies. J Neurol 263(12):2361–2368
60. Shen Y, Jian W, Li J, Dai T, Bao B, Nie H (2018) Bilateral wallerian degeneration of the middle cerebellar peduncles secondary to pontine infarction: A case series. J Neurol Sci 388:182–185
61. Konno T, Broderick DF, Tacik P, Caviness JN, Wszolek ZK (2016) Hypertrophic olivary degeneration: a clinico-radiologic study. Parkinsonism Relat Disord 28:36–40
62. Bertrand A, Leclercq D, Martinez-Almoyna L, Girard N, Stahl J-P, De-Broucker T (2017) MR imaging of adult acute infectious encephalitis. Med Mal Infect 47(3):195–205

63. Breville G, Koralnik IJ, Lalive PH (2021) Brainstem progressive multifocal leukoencephalopathy. Eur J Neurol 28(3):1016–1021
64. Hodel J, Outteryck O, Dubron C, Dutouquet B, Benadjaoud MA, Duhin E et al (2016) Asymptomatic progressive multifocal leukoencephalopathy associated with natalizumab: diagnostic precision with MR imaging. Radiology 278(3):863–872
65. Wijburg MT, Witte BI, Vennegoor A, Roosendaal SD, Sanchez E, Liu Y et al (2016) MRI criteria differentiating asymptomatic PML from new MS lesions during natalizumab pharmacovigilance. J Neurol Neurosurg Psychiatry 87(10):1138–1145
66. Sandhu S, Soule E, Fiester P, Natter P, Tavanaiepour D, Rahmathulla G et al (2019) Brainstem diffuse axonal injury and consciousness. JCIS 28(9):32

Publisher's Note Springer Nature remains neutral with regard to jurisdictional claims in published maps and institutional affiliations.